Lawrence Berkeley Laboratory
UNIVERSITY OF CALIFORNIA

Submitted to Physical Review C

URANIUM NUCLEAR REACTIONS AT 900 MeV/NUCLEON

D.E. Greiner, H. Crawford, P.J. Lindstrom,
J.M. Kidd, D.L. Olson, W. Schimmerling,
and T.J.M. Symons

October 1984

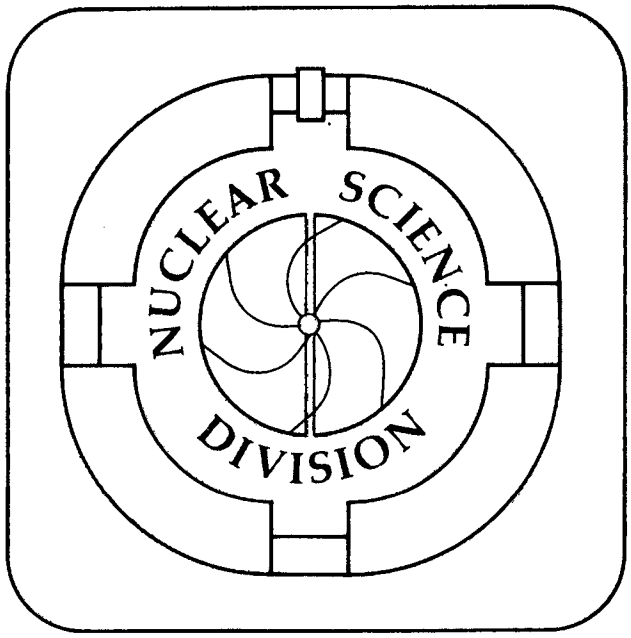

Prepared for the U.S. Department of Energy under Contract DE-AC03-76SF00098

DISCLAIMER

URANIUM NUCLEAR REACTIONS AT 900 MeV/Nucleon

D. E. Greiner, H. Crawford[*], *P. J. Lindstrom,*
J. M. Kidd[**], *D. L. Olson, W. Schimmerling, T. J. M. Symons*

Lawrence Berkeley Laboratory, Berkeley, CA, 94720
[*]Space Sciences Laboratory,
University of California,Berkeley, CA 94720
[**]Naval Research Laboratory,Washington DC, 27305

PACS number 25.70.nP

This work was supported by the Director, Office of Energy Research, Division of Nuclear Physics at the Office of High Energy and Nuclear Physics of the U. S. Department of Energy under Contract DE-AC03-76SF00098 and NASA Grant NGR 05-003-513

ABSTRACT

The cross sections for break-up of ^{238}U in targets ranging from H to Pb are presented. Fragmentation modes measured include: total charge changing, fission, and central collision. The charge changing cross sections are compared with black disk geometrical and Glauber models. The central collision cross section rises as the mass of the target and reaches 20% of the measured cross section for uranium on a lead target. The limiting fragmentation hypothesis is satisfied for targets heavier than hydrogen. For uranium-uranium central collisions this data predicts a cross section of 2.5 barns.

INTRODUCTION

The acceleration of ^{238}U to relativistic energies at the BEVALAC has opened a new area of study.[1,2] Very little is known experimentally about the physics of such highly charged energetic particles. In order to begin to study the reactions in this realm the basic questions about reaction rates and modes of fragmentation must be answered.

During an experiment to measure the equilibrium charge distributions of relativistic uranium in matter, a few hours of beam time were devoted to the first measurements of the nuclear cross sections of uranium on various elemental targets. The goal of the experiment was to measure the target mass dependence of the reaction cross section, the fission cross section and, to obtain some information of the probability of central collisions. Such information tests the geometric models of the reaction mechanism, the limiting fragmentation hypothesis and also provides necessary information for the design of future accelerators and experiments.

APPARATUS and ANALYSIS

The uranium ions were injected into the BEVATRON at charge state +68 from the SUPERHILAC. The beam was accelerated to 960 MeV/nucleon, extracted and delivered to the experimental area. The ions then passed out of the vacuum chamber through a 55mg/cm^2 window and struck the experimental apparatus shown in Fig. 1a.

Two 1mm thick by 4.6cm diameter position sensitive solid state detectors (D1,D2) were used to identify the beam charge and position before the target. These detectors assured us that fragments made in the window and the air of the cave were not used in the cross section determinations. The position determination required that the beam particles selected for reaction measurements be centered on the targets. After the target, there was a solid state detector telescope (D3-10)consisting of two 1mm thick by 4.6cm diameter detectors and seven 5mm thick by 7.6cm diameter detectors to determine the type of reaction which had taken place. Detector spacing was typically 8-9mm; the target was 2cm behind the second PSD and 12.5cm in front of the D3-10 telescope. All particles produced in the target traveling within 10.4 degrees of the beam direction hit the D3 detector. Targets used ranged from CH2 to Pb and are listed in Table 1.

Data was collected whenever D1 and D2 were in coincidence and above one half of the nominal beam pulse height. The signals from the detectors were amplified and then digitized using LeCroy 2259 peak sensing analog to digital units in Camac. Data was routed through the standard Heavy Ion Spectrometer System of data collection and diagnostics.[3]

The pulse height spectrum in D3 when D1 and D2 record a 92U beam particle centered on a Cu target is shown in Fig. 1b. Basic to understanding the features of this data is the fact that at this energy the projectile fragments are

moving at very close to beam velocity. Because the projectile fragments move forward in a narrow cone, the detectors downstream of the target record the total energy loss of all projectile fragments from the reaction. Thus the signal is proportional to the sum of the charges of the fragments squared. Since our trigger scheme accepts un-interacted events we have the known charge of the beam to calibrate the energy seen in the detectors. A useful variable is the effective charge of the particle or particles after the reaction. Because dE/dX is proportional to Z^2 at constant velocity the square root of the energy deposit is proportional to the charge of the particle. We define the effective charge, Z^*, as the square root of the energy deposit normalized so the Z^* of the beam is 92. In our case there is usually more than one particle present, however, Z^* is usually dominated by one or two particles. For instance, a Z^* =20 event could be produced by: one Z=20 particle, two Z=14.1 particles, one Z=18+76 protons, 100 alpha particles, 400 protons, etc. Because we have only 92 charges available it is clear that only cases where one or two multiply charged particles dominate the signal are possible. At the higher Z^* regions the leading charges dominate because of the Z^2 dependence of dE/dX.

With these considerations in mind let us turn to Fig. 2. Here we have plotted the Z^* spectra for approximately equal numbers of reactions produced in the various targets. The spectrum for the hydrogen target was obtained by subtracting an appropriate number of carbon target events from the CH2 data. We have cut off the Z^* scale at Z^*=86 to avoid confusion with the tails of the uninteracted beam signals. As the target mass increases the qualitative change in the nature of the signal is striking. First, the peak at about Z^*=65, is a clear indication that fission has taken place because two particles of about Z=46 would have a Z^* of 65. This semi-raw data then shows us in a qualitative fashion that the reaction of uranium with hydrogen is dominated by fission and that the

fission process becomes less and less prominent as the target mass increases.[4] Also we see that there is a drastic increase of low Z^* events as the target mass increases. Ultimately this feature competes with fission as the most favored topology in the reaction. These low Z^* events are naturally interpreted as violent events where the bulk of the projectile is broken up in the reaction. The probability of catastrophic collisions is of more than passing interest,as such events are the first place where one expects new phenomena to be exhibited. This is due to the possibility of high nuclear temperatures and densities. In the following sections we will quantify the reaction modes we have defined here.

CHARGE CHANGING CROSS SECTION

At the right of the graph in Fig. 1b is the peak produced by the uninteracted beam which defines the signal produced by the detector for Z=92. The difference in the integrated beam flux before and after the target measures the cross section for charge change (after suitable subtraction of target out contributions). Because of this fact, this experiment is insensitive to neutron removal. We quote the charge changing cross section which is equal to the reaction cross section minus all non-charge changing reactions. Below we estimate this difference. The analysis methods are essentially the same as those used in an earlier experiment described in Ref. 5. The results for the various targets are listed in Table 1. One further target mass (^{28}Si) is made available by looking at the decrease of beam flux in the telescope itself.

In Fig. 3, we compare the data to the standard geometrical overlap model. The overlap model has the following form:

$$\sigma=\pi R_0^2(A_T^{1/3}+A_B^{1/3}-\delta)^2$$

where we take R_0=1.4×10^{-13} cm and δ=1.0 which are values found to fit heavy ion reactions in the region of A_B=12-56.[5,6] The fit is quite poor. The overprediction at low target masses is probably due to nuclear transparency effects. At

target masses above 40 amu the underprediction may be explained by the fact that coulomb processes become significant. Coulomb excitation followed by neutron emission or fission is significant for the targets Cu and heavier. It is the electromagnetically induced fission that affects the signal in this experiment. We have calculated this contribution using measured photonuclear cross sections and the Weizsacker-Williams virtual photon spectrum.[7,8] For the Cu, Ta and Pb targets the electromagnetically induced fission contributions are .23, 1.16 and 1.49 barns, respectively. Subtracting these values from the data points in Fig. 3 indicates that the geometric model is adequate for the nuclear part of the cross section on targets heavier than hydrogen. Further insight is found by comparison with the soft-spheres model of Karol.[9] This model is a closed form approximation to the Glauber optical formalism, it uses tapered nuclear density distributions and should account for the transparency effect. In applying this model we have added our calculation of the electromagnetic contributions and allowed the nucleon-nucleon cross section input parameter to be variable. The resultant best fit value of 20mb is an effective nucleon-nucleon cross section for the charge changing portion of the reaction cross section. The open triangles in Fig. 3 show the agreement is good over the entire range of target masses. We thus conclude that the optical model adequately predicts the cross section as long as the electromagnetic component is added. In this model the difference between our effective nucleon-nucleon cross section and the experimental value of 40mb for this energy range is due to unobserved non-charge changing channels such as neutron removal and nuclear excitation. If this interpretation is true; then the nuclear reaction cross section is larger than the charge changing cross sections reported here by 13% for a hydrogen target to 6% on the lead target.

Because the energy loss while passing through the detectors is appreciable

the silicon target measurement is available as a function of beam energy. The energy dependence of the charge changing cross section of uranium on silicon is negligible at the level of our statistics(10%) over the range 150-930 MeV/nucleon. This behavior would be expected if the reaction is primarily determined by geometrical effects as we have concluded above from the success of the Glauber approach.

FISSION CROSS SECTION

The peaks at half the beam pulse height are caused by the events where fission of the uranium took place(Fig. 1). When fission takes place the fragment charges are both close to half the uranium charge. Thus we expect to see a signal $(Z/2)^2+(Z/2)^2=Z^2/2$. The asymmetric events broaden the peak and a small component of Z=1,2 fragments shift the peak slightly toward lower pulse heights. The fission cross sections were calculated by integrating the events in the area of the fission peaks, subtracting background from target out and also subtracting the continuum produced by fragmentation type events producing a single highly charged fragment. The continuum was estimated by smoothly connecting the continuum areas on each side of the fission peak. The values of the fission cross sections are tabulated as a function of target mass in table 1. The fission cross section of ^{238}U when bombarded with 1GeV protons has been measured previously using emulsion techniques by Bochagov et al.[10] Their value of 1.4±.1 barns agrees with our value of 1.2±.13. Thus we have some corroboration to engender confidence in our method of extracting the fission portion of the reaction. If the electromagnetic contribution to the fission cross section is subtracted for the heavier targets we see that the nuclear induced component is almost constant as target mass increases. In Fig. 3, we have plotted the nuclear component and fit it to a power law in target mass for targets heavier than hydrogen. The resultant power (.08±.06) is consistent with similar data for

peripheral reactions seen for lighter beams.[11] This target dependence is also predicted by the Glauber model.[9,11]

CENTRAL COLLISION CROSS SECTION

The concept of calculating the cross sections of prominent features of the data was also applied to the peak at low pulse heights. This peak corresponds to the break up of the uranium into many low charged fragments. We call the cross section for this feature the central collision cross section. The definition of the peak is chosen to be the pulse height corresponding to the sum of the fragment charges squared being less than 400. This requirement could be satisfied by a single fragment of z=20 or more probably an event containing a single fragment in the range z=10-15 and accompanying z=1 and 2 particles. This definition of centrality is slightly more restrictive than that used in an analysis of streamer chamber data.[12] It is more restrictive in the sense that we see 20% central collisions for U+Pb while the streamer chamber results give 25% for Ar +Pb. The central collision cross section is listed for the various targets in Table 1. In the geometrical model our central cross section corresponds to an impact parameter of 6 fermi for Pb +U. With the exception of the carbon target point the central collision cross section increases as A of the target. This strengthens our definition of "central" for this feature of the reaction cross section. Qualitatively, what appears to be happening is that the carbon target is not large enough to destroy the uranium while the heavier targets can produce destruction whenever they overlap the uranium completely. Thus although the impact parameter is not zero, the central collisions as defined here are very destructive of the uranium and the linear dependence on target mass indicated that all target nucleons take part in this dramatic process. It is important from the viewpoint of the design of colliding beam machines that the central part of the cross section where the quark-gluon plasma may be produced is estimated from

this data to be 2.5 barns for U-U collisions!

LIMITING FRAGMENTATION

The limiting fragmentation hypothesis states that at high enough energies the cross section for fragmentation into the various channels is independent of target.[13] This concept has been tested for heavy ion reactions and been found valid for beams as heavy as iron and targets from Be to U.[11] The Glauber model predicts this factorization for peripheral reactions. [11] With our present data it is possible to extend the test to hydrogen target and uranium beam. We do this by looking at the target dependence of the nuclear part of the fission channel relative to the other channels dominated by a high leading charge. These channels are defined by being that part of the cross section that is not fission and also not central. Thus we just subtract the fission cross section and the central cross section from the total charge changing cross section. This ratio is plotted in Fig. 4 as a function of target mass. It is clear that for the C to Pb targets the ratio is constant. However, there is a large relative excess in the fission channel for the hydrogen target. We attribute this to the fact that it takes over 1.7GeV to completely disassociate uranium into its constituent nucleons, thus many channels just are not open even if the proton deposits all of its energy in the uranium. The uranium reactions at 900MeV/nucleon obey limiting fragmentation with the exception of the hydrogen target where the large total binding energy of the uranium leads to deviations.

CONCLUSIONS

These charge changing measurements indicate that the nuclear part of the uranium reaction cross section is well explained using the soft spheres model for all target masses.[9] At target masses, Cu and above, Coulomb effects are substantial and cannot be ignored. The non-central part of the fragmentation cross

section factors as predicted by the limiting fragmentation hypotheses for targets heavier than hydrogen. The soft spheres model also correctly predicts factorization and gives the observed target dependence for the peripheral part of the cross section.[9,11] The violation of limiting fragmentation for the hydrogen target is attributed to the large binding energy of uranium. The portion of the nuclear reaction cross section responsible for non-charge changing reactions is in the region of 6 to 13 %. The central collisions increase as A of the target and reach 20% of the reaction cross section for the larger targets.

This work was supported by the Director, Office of Energy Research, Division of Nuclear Physics at the Office of High Energy and Nuclear Physics of the U.S. Department of Energy under Contract DE-AC03-76SF00098 and NASA Grant NGR 05-003-513

REFERENCES

1. H. H. Heckman, Y. J. Karant, and E. M. Friedlander, Science, 217, 1137 (1982)
2. E. M. Friedlander, H. H. Heckman, Y. J. Karant, Phys. Rev. C 27, 2436 (1983)
3. Charles McParland, IEEE Transactions on Nuclear Science, Vol. NS-30, No. 5, 3953 (1983)
4. The shape of the fission peak for the tantalum target is broader due to the straggle in energy produced by the thick tantalum target
5. G. D. Westfall, Lance W. Wilson, P. J. Lindstrom, H. J. Crawford, D. E. Greiner, H. H. Heckman, Phys. Rev. C 19, 1309 (1979)
6. H. H. Heckman, D. E. Greiner, P. J. Lindstrom and H. Shwe Phys. Rev. C 17, 1735 (1978)
7. D. L. Olson, B. L. Berman, D. E. Greiner, H. H. Heckman, P. J. Lindstrom, G. D. Westfall and H. J. Crawford, Phys. Rev. C24, 1529 (1981)
8. J. T. Caldwell, E. J. Dowdy, B. L. Berman, R. A. Alvarez, and P. Meyer, Phys. Rev. C21, 1215 (1980)
9. Paul J. Karol, Phys. Rev. C, 11,1203 (1975)
10. B. A. Bochagov et. al., Sov. J. Nucl. Phys. 28(2), 291 (1978)
11. D. L. Olson, B. L. Berman, D. E. Greiner, H. H. Heckman, P. J. Lindstrom and H. J. Crawford, Phys. Rev. C28, 1602 (1983)
12. H. Ströbele, R. Brockman, J. W. Harris, F. Riess, A. Sandoval, H. G. Pugh, L. S. Schroder, and M. Maier, Phys. Rev. C27,1349 (1983)
13. J. Cugnon and R. Sartor, Phys. Rev. C21, 2342, (1980)

CAPTIONS

TABLE 1

Measured charge changing, fission and central cross sections in barns for targets H to Pb. The charge changing cross section requires that the beam lose more than one charge unit in the reaction; this quantity is close to the reaction cross section. Fission cross section is for fission of ^{238}U. The central collision cross section is a measure of the strength of the destruction peak as defined in figure 1, namely, that the dE/dX observed after the reaction is less than that which would be made by a single fragment of charge 20. This feature of the cross section varies as A of the target.

FIGURE 1

[a] Experimental apparatus: Detectors D1-4 are 1.02mm thick, position sensitive solid state detectors with resistive read out. Detectors D5-10 are 4.72mm thickness solid state detectors. The detectors down stream of the target subtend an opening angle of 21 degrees.

[b] Typical pulse height spectrum for detector D3 with the Cu target in place. The features common to all targets are: the large peak of un-interacted beam, the fission peak near dE/dX=half of the beam value and the central collision peak occurring at low dE/dX indicating loss of most of the highly charged particles in the forward direction. The cuts to determine the charge changing, fission, and central cross sections are shown.

FIGURE 2

The effective charge $Z^*=\sqrt{\sum Z_i^2}$ of the reaction products of uranium on targets from H to Pb. The beam peaks have been suppressed. The histograms for each target contain equal numbers of reactions in order to stress the change in the reaction topology with target mass. Note the rapid rise of the central collision peak at low Z^* for the targets heavier than carbon.

FIGURE 3

Charge changing, fission and central collision cross sections plotted as a function of target mass for a uranium projectile at 900 MeV/nucleon. Open triangles indicate the calculated charge changing cross section using the closed form optical model plus electromagnetic corrections. Labeled curves are geometric and power law fits to the data. The nuclear part of the fission cross section is indicated by the circled x points. The central collision component rises as A_T and reaches 20% of the measured cross section for the lead target.

FIGURE 4

The ratio of the nuclear part of the fission cross section σ_{FN} to the cross section for producing large fragments $\sigma_{\Delta Z}-\sigma_F-\sigma_C$ plotted as a function of target mass. The constant value excluding the hydrogen point indicates the cross section factors.

TABLE 1

target material (amu)	charge changing cross section (barns)	fission cross section (barns)	central collision cross section (barns)	energy range (MeV/N)
H	1.72 ± .18	1.21 ± .13	.000 ± .003	840-920
C	3.23 ± .33	0.82 ± .09	.022 ± .005	840-920
Al	4.20 ± .43	1.10 ± .13	.25 ± .03	870-920
Si	3.85 ± .40	———	———	150-920
Cu	5.45 ± .56	1.27 ± .14	.74 ± .08	850-920
Ta	8.23 ± .84	2.02 ± .22	1.90 ± .20	680-920
Pb	9.69 ± 1.0	2.73 ± .20	2.00 ± .23	840-920

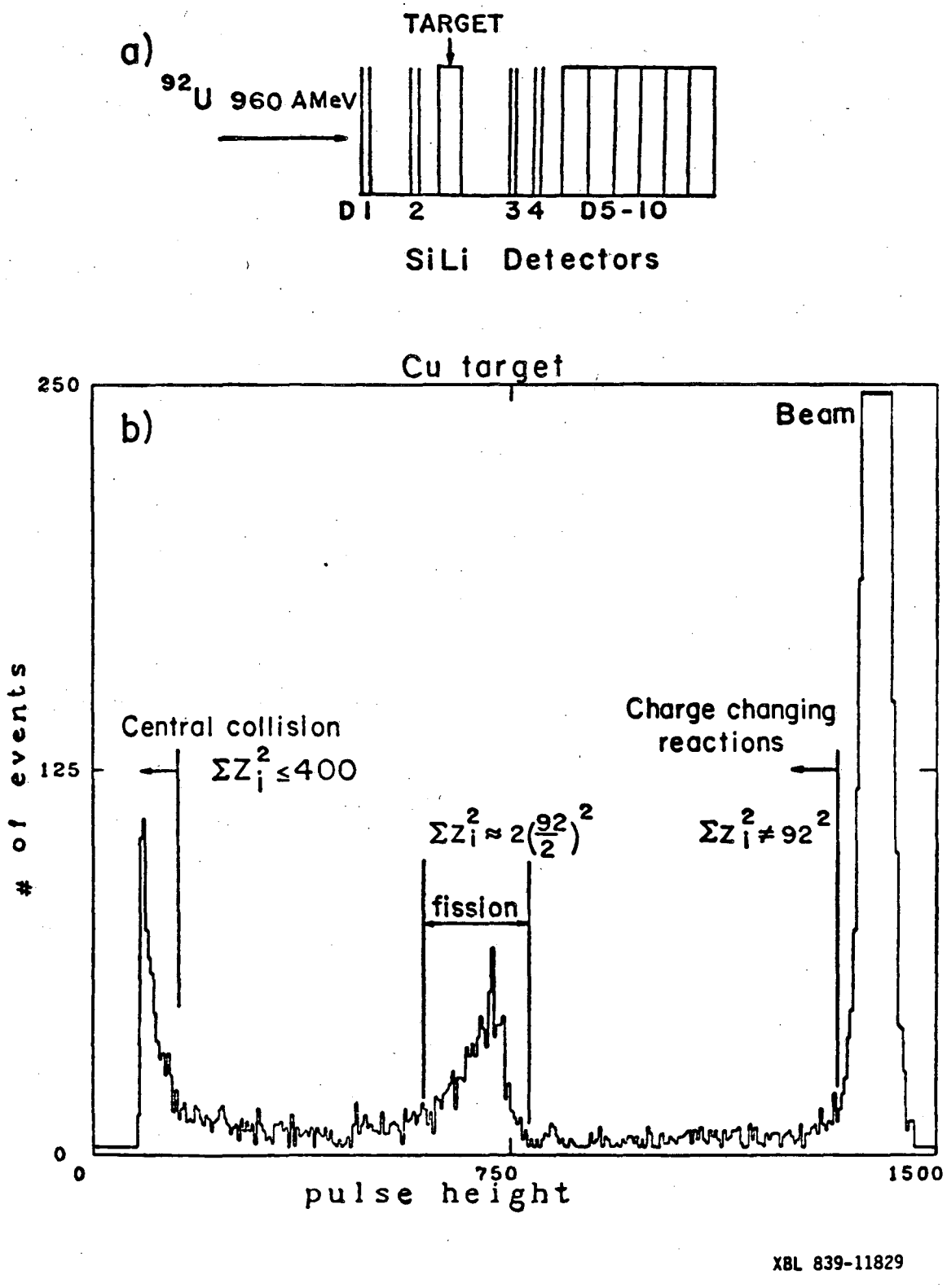
a)
^{92}U 960 AMeV
TARGET
D1 2 3 4 D5-10
SiLi Detectors
b)
Cu target
Beam
Central collision
$\Sigma Z_i^2 \leq 400$
$\Sigma Z_i^2 \approx 2(\frac{92}{2})^2$
fission
Charge changing reactions
$\Sigma Z_i^2 \neq 92^2$
# of events
250
125
0
0
750
1500
pulse height
XBL 839-11829

FIG. 1

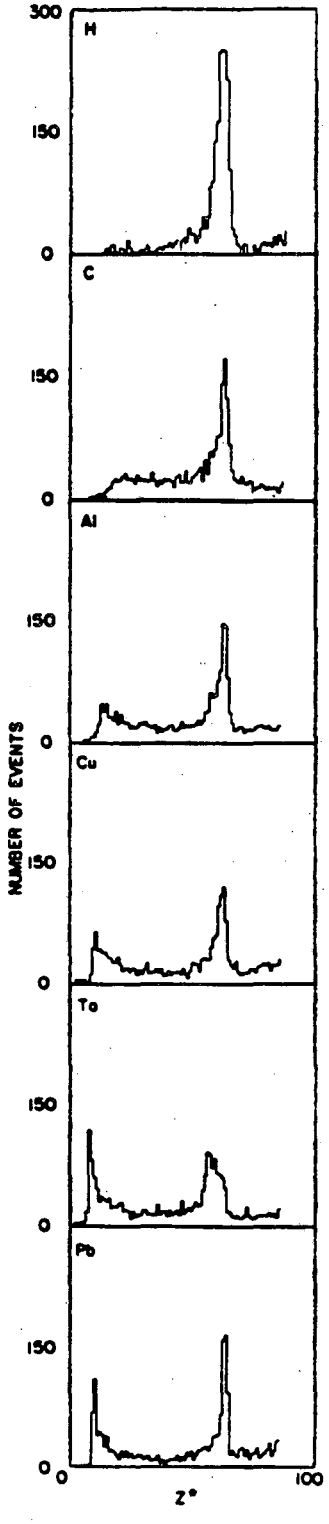

XBL 839-11825

FIG. 2

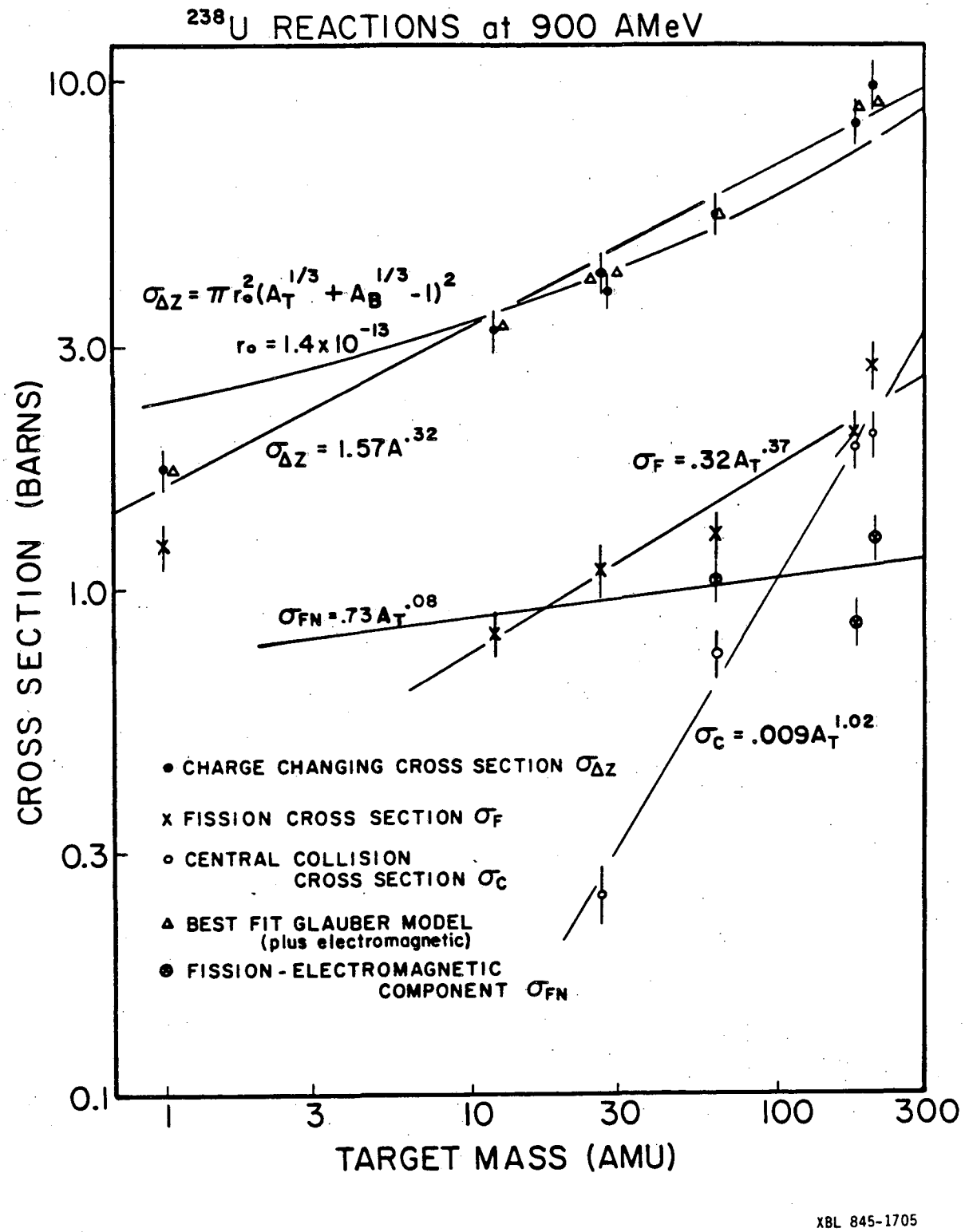
^{238}U REACTIONS at 900 AMeV
CROSS SECTION (BARNS)
10.0
3.0
1.0
0.3
0.1
1
3
10
30
100
300
TARGET MASS (AMU)
$\sigma_{\Delta Z} = \pi r_o^2 (A_T^{1/3} + A_B^{1/3} - 1)^2$
$r_o = 1.4 \times 10^{-13}$
$\sigma_{\Delta Z} = 1.57 A^{.32}$
$\sigma_F = .32 A_T^{.37}$
$\sigma_{FN} = .73 A_T^{.08}$
$\sigma_C = .009 A_T^{1.02}$
• CHARGE CHANGING CROSS SECTION $\sigma_{\Delta Z}$
x FISSION CROSS SECTION σ_F
o CENTRAL COLLISION CROSS SECTION σ_C
Δ BEST FIT GLAUBER MODEL (plus electromagnetic)
⊛ FISSION - ELECTROMAGNETIC COMPONENT σ_{FN}
XBL 845-1705

FIG. 3

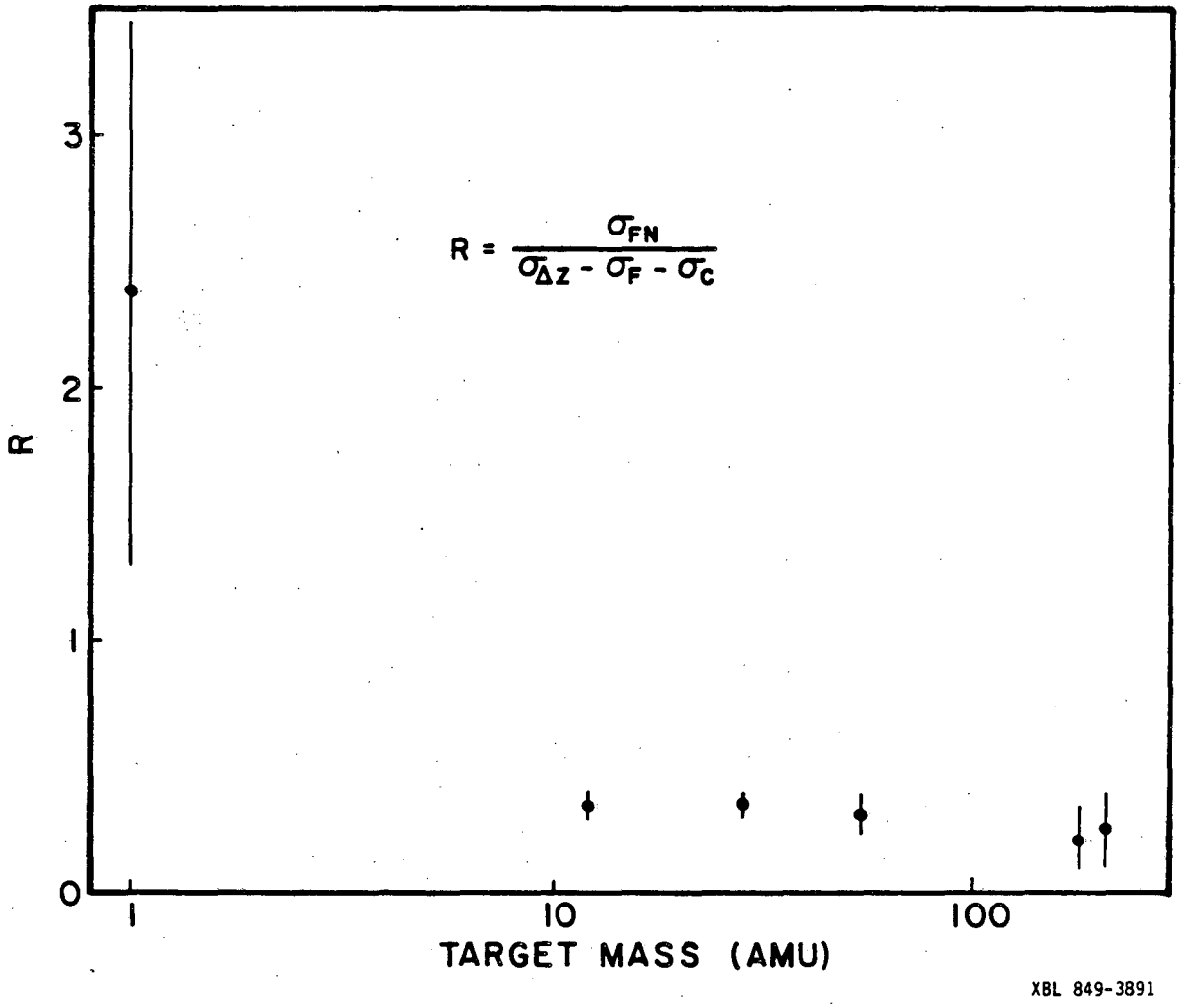
$R = \frac{\sigma_{FN}}{\sigma_{\Delta Z} - \sigma_F - \sigma_C}$
R
3
2
1
0
1
10
100
TARGET MASS (AMU)
XBL 849-3891

FIG. 4

TECHNICAL INFORMATION DEPARTMENT
LAWRENCE BERKELEY LABORATORY
UNIVERSITY OF CALIFORNIA
BERKELEY, CALIFORNIA 94720